

# PROPOSAL FOR NON-DESTRUCTIVE ELECTRON BEAM DIAGNOSTIC WITH LASER-COMPTON BACKSCATTERING AT THE S-DALINAC \*

M. Meier<sup>†</sup>, M. Arnold, J. Enders and N. Pietralla

Technische Universität Darmstadt, Department of Physics,  
Institute for Nuclear Physics, Schlossgartenstr. Darmstadt, Germany

## Abstract

To recover a large fraction of energy from the accelerator process in an energy-recovery linac, experiments, secondary-beam production, and beam diagnostics must be non-destructive and/or, hence, feature a low interaction probability with the very intense electron-beam. Laser-Compton backscattering can provide a quasi-monochromatic highly polarized X-ray to  $\gamma$ -ray beam without strongly affecting the electron beam due to the small recoil and the small Compton cross-section. Highest energies of the scattered photons are obtained for photon-scattering angles of  $180^\circ$ , i. e., backscattering. A project at TU Darmstadt foresees to synchronize a highly repetitive high-power laser with the Superconducting DArmsstadt electron LINear ACcelerator S-DALINAC, capable of running in energy recovery mode to realize a laser-Compton backscattering source with photon beam energy up to 180 keV. The source will be first used as a diagnostic tool for determining and monitoring key electron-parameters, in particular energy and the energy spread at the S-DALINAC operation. Results are foreseen to be used for optimizing the design of laser-Compton backscattering sources at energy-recovery linacs.

## INTRODUCTION

Bright, monochromatic and tunable X-Ray to  $\gamma$ -ray sources of very small spot size are necessary for a wide range of applications from diffraction and spectroscopy in material and radiography and tomography biomedical science [1, 2] to photo nuclear reactions [3] like nuclear resonance fluorescence or photo fission [4]. Photon beams with energies in the range from 1 keV to 200 keV are mostly generated in synchrotrons with undulators. These facilities usually have the disadvantage that they are very large and would require electrons in the high GeV range for higher photon energies. For these cases, more and more Compton backscattering sources have become increasingly interesting [5]. By combining small storage rings and novel laser systems, the size of laser-Compton backscattering (LCB) sources can be reduced to less than  $100\text{ m}^2$  [6]. But also with conventional accelerators photon energies far above 1 MeV can be generated. Here the inverse Compton effect is used, where a photon, at an angle of  $180^\circ$ , is scattered by a relativistic electron, thereby gaining energy. The photons

get Lorentz boosted in the direction of electrons, giving the characteristic radiation cone, with an opening angle proportional to  $1/\gamma$  and the typical maximum energy in head-on geometry [7] of  $E_\gamma = 4\gamma^2 E_L$  with the laser photon energy  $E_L$  starting from infrared up to ultraviolet and the Lorentz factor  $\gamma = E_e/m_e c^2$ , where  $c$  is the speed of light and  $m_e$  is the rest mass of the electron. Thus, it takes electrons with an energy of approx. 240 MeV to scatter laser photons in the infrared region to produce photons with an energy greater than 1 MeV. In most cases, due to the use of lasers, the energy of the incident photon is much less than the rest energy of the electron, making the recoil of the electrons negligible. Also, the effective cross section of the scattering is very small, which keeps the probability of multiple scattering low. Therefore LCB is perfect suited as in beam experiment at energy-recovery linacs (ERL) [7]. ERL-based LCB sources are expected to feature higher brightness from high duty factor and increased beam currents with low emittance and energy spread. Another useful aspect of LCB is the ability to monitor the electron beam non-destructively in its energy and energy spread [8–10].

This contribution focuses on the proposed design, feasibility, and investigation of an LCB source at the thrice-recirculating S-DALINAC, with the possibility to operate as ERL [11].

## COMPTON BACKSCATTERING

Compton backscattering occurs when a photon with energy  $E_L$  hits a relativistically moving electron with energy  $E_e$  and is backscattered. Energy is transferred from the electron to the photon. The recoil factor  $X = (4E_e E_L)/(m_e^2 c^4)$  [12] indicates how strong the energy loss and thus the influence on the electrons is. The energy of the scattered photons  $E'_L$  can be calculated by [13]

$$E'_L = \frac{(1 - \beta \cos(\theta_i))E_L}{(1 - \beta \cos(\theta_s)) + (1 - \cos(\theta_r))\frac{E_L}{E_e}} \quad (1)$$

for electrons with  $\beta = v/c$ ,  $v$  the average speed of the electrons,  $c$  the speed of light,  $\theta_i$  the angle between the incident photons and electrons,  $\theta_s$  the scattering angle of the scattered photons and the electron beam axis and  $\theta_r = \theta_i - \theta_s$  the reflecting angle between incident and scattered photons. From eq. (1) it can be concluded that the desired photon energy can be achieved by adjusting both the original electron and photon energy. However, this can also be achieved in a small ranges by an angle-dependent positioning of the target or detector to the beam axis of the scattered photons, a variation of  $\theta_r$ . The highest photon energy can be achieved

\* Work supported in part by the state of Hesse within the research cluster ELEMENTS (project ID 500/10.006) and the LOEWE research cluster Nuclear Photonics and by DFG through GRK 2128 "Accelence" and Inst163/308-1 FUGG.

<sup>†</sup> m.meier@ikp.tu-darmstadt.de

by a head-on collision  $\theta_i = 180^\circ$ , see Eq. (1). Looking at the detection angel of  $\theta_r = 0^\circ$  the Eq. (1) simplifies to

$$E'_L{}^{max} = \frac{4\gamma^2 E_L}{1 + 4\gamma^2 (E_L/E_e)} = \frac{4\gamma^2 E_L}{1 + X} \quad (2)$$

including the recoil  $X$  [12]. By using lasers with photon energies in the visible range, we are in the limit region  $X \ll 1$ , i.e. in the Thomson regime.

The energy bandwidth  $\Delta E'_L/E'_L$  of the scattered photons depends on many parameters of the electron and laser beam. First of all, the collimation angle  $\theta_s^{max}$ , described by the acceptance angle  $\Psi = \gamma_{CM} \theta_s^{max} \ll 1$  with the Lorentz factor in the center of mass (CM) system [12],

$$\gamma_{CM} = \frac{E_{tot}^{LAB}}{E_{CM}} \approx \frac{E_e + E_L}{\sqrt{4E_e E_L + m_e^2}} \quad (3)$$

assuming  $E_e \gg E_L$  and  $\gamma \gg 1$ . The Bandwidth also depends on, the relative energy spread  $\delta\gamma/\gamma$ , the normalized emittance  $\epsilon_n$  and the rms spot size  $\sigma_e$  (Gaussian phase space distribution (GPSD)) at the interaction Point (IP) of the electron beam, the laser bandwidth  $\Delta E_L/E_L$ , the laser wavelength  $\lambda_0$ , the laser focal spot size  $\omega_0$  (GPSD) at IP, the beam quality factor  $M^2$  and the laser parameter  $a_0 = 6.8(\lambda_0 \omega_0) / \sqrt{(U_L(J)) / (\sigma_r(\text{ps}))}$ , with  $U_L(J)$  being the lase pulse energy in Joule and  $\sigma_r(\text{ps})$  being the pulse length in pico seconds. The relative scattered photon bandwidth [12] is given by

$$\frac{\Delta E'_L}{E'_L} = \frac{\sqrt{\left[ \frac{\Psi^2 / \sqrt{12}}{1 + \Psi^2} + \frac{\bar{P}^2}{1 + \sqrt{12} \bar{P}^2} \right]^2 + \left[ \left( \frac{2+X}{1+X} \right) \frac{\Delta\gamma}{\gamma} \right]^2}}{\sqrt{\left[ \frac{1}{1+X} \frac{\Delta E_L}{E_L} \right]^2 + \left[ \frac{M^2 \lambda_0}{2\pi \omega_0} \right]^4 + \left[ \frac{a_0^2 / 3}{1 + a_0^2 / 2} \right]^2}} \quad (4)$$

with the term  $\bar{P} = (\sqrt{2}\epsilon_n) / (\sigma_e \sqrt{1+X})$ . The most influence on the relative bandwidth is given by the first term, resulting in a high dependency to the collimation angle and the electron beam parameters, i.e. energy, rms size and emittance.

The last important parameter for the design of a LCB source is the expected photon flux. This results from the luminosity  $\mathcal{L}$  multiplied by the Compton cross section  $\sigma$  [13]. For head-on collisions the number of scattered photons per second is given by

$$\mathcal{N} = \mathcal{L} \sigma = \frac{N_e N_L r}{2\pi (\sigma_e^2 + \sigma_L^2)} \sigma \quad (5)$$

with  $N_e$  and  $N_L$  the number of electrons and photons respectively. For  $\lim_{X \rightarrow 0} \sigma = \sigma_T (1 - X)$  [12] the Compton cross section becomes the Thomson cross section  $\sigma_T = 66.5 \text{ fm}^2$ .

## LASER-COMPTON BACKSCATTERING AT S-DALINAC

### The S-DALINAC

The S-DALINAC delivers energies of up to 130 MeV with average currents of up to 20  $\mu\text{A}$  at this energy with a repeti-

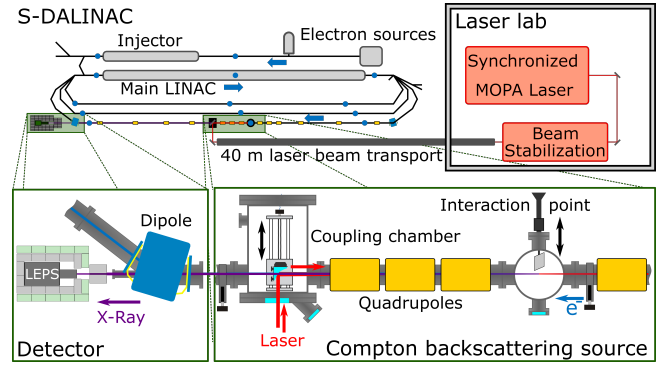


Figure 1: Schematic floor-plan of the S-DALINAC. The LCB-Source is placed in the third recirculation beam line, consisting of two vacuum chambers, the coupling chamber and the interaction chamber. The generated X-ray beam are detected by a LEPS.

tion rate of 3 GHz. It was operated as first ERL in Germany in 2017 [11], and was successfully operated as multi-turn ERL in 2021 [14, 15]. It is planned to install the LCB setup in the third recirculation beam line of the accelerator, where the electrons will reach an energy of up to 99 MeV and thus we can expect photons of up to 180 keV, see Fig. 1.

These photons will be detected by a Low-Energy Photon Spectrometer (LEPS). The laser system is set up further away from the accelerator due to possible damage from radiation. Therefore, it is necessary to guide the laser beam to the interaction point via a approx. 40 m long beam transport.

### Coupling Chamber Design

From the theoretical description of the Compton effect, we know that the maximum possible energy, see Eq.(1), and the maximum possible flux, see Eq. (5) and [13], are achieved by a head-on collision of the two beams. Moreover, it simplifies the timing synchronization of the laser pulses with the electron bunches as well as the theoretical consideration and the back-calculation from the scattered photon energy to the electron energy, for later diagnostics. It is necessary to get the laser beam on the beam axis of the electrons for a head-on collision. For this purpose, an off-axis parabolic mirror will be used. It deflects the laser beam by  $90^\circ$  and focuses it with a focal length of 2 m on the IP to a focal spot size of  $\omega_0 = 100 \mu\text{m}$  without aberration. This provides a Gaussian shaped, high-intensity focus with long Rayleigh length  $z_R = (\pi \omega_0^2) / (M^2 \lambda_0)$  of approx 23.5 mm. The electron beam and also the scattered photons can pass the parabolic mirror through a small hole of  $d_0 = 1.7 \text{ mm}$ . For the laser beam, this means an intensity loss of approx. 2% with a beam size of  $\omega_L = 8.5 \text{ mm}$  at the mirror. This can be estimated with  $R = \exp[-2(d_0/2\omega_L)^2]$ . The electron-beam transmission was tested during a beam time with a dummy version of the mirror and a beam deposition of  $0.67\% \pm 0.56\%$  was measured. The designed coupling chamber is shown in Fig. 2. The five-axis optical table and the linear optical stage are for pre-alignment of

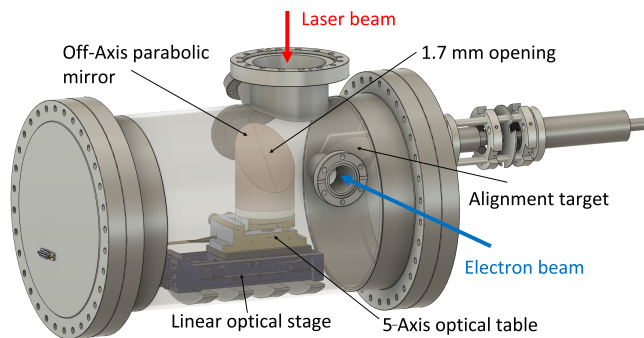


Figure 2: CAD drawing of the coupling chamber. With the off-axis parabolic mirror, the laser beam is antiparallel overlapped with the electron beam and focused. The mirror has a hole so that the electron beam can pass through. The transparent barrel is only for illustration purposes.

the parabolic mirror to the electron axis, and to extract the mirror from the beam axis. An alignment target checks the correct overlap of the two beams in advance. The active adjustment and stabilisation of the laser focus position during operation of the LCB source will be done by additional mirrors in front of the parabolic mirror and by an exact copy of the actual beam-line with a second identical parabolic mirror with which the light is focused on a position sensitive quadrant detector.

### Laser System and Laser Beam Simulation

Since the first design approach of the LCB source at the S-DALINAC should have a geometry as simple as possible and be flexible in position, each pulse of the laser is superimposed only once with an electron bunch. The laser has to be powerful enough to deliver a sufficient flux to be able to detect the scattered photons. In addition, a high repetition rate is preferred, since the S-DALINAC runs at a frequency of 3 GHz. To obtain a good intrinsic bandwidth through the laser, it is also necessary to have the lowest possible beam quality factor  $M^2$  and a small energy bandwidth  $\Delta E_L/E_L$ . Furthermore, a good synchronisation of the laser system and the accelerator as well as a stable long-term operation is necessary. Ytterbium-based laser systems have proven suitable for this purpose. These have a wavelength of 1030 nm and an average output power of >100 W at around 100 kHz repetition rate. This results in a pulse energy in the range of 1 mJ. The  $M^2$  factor is below 1.3 and the energy bandwidth is close to the Fourier limit for 3 ps long pulses.

The complete optical setup including beam transport of 40 m and off-axis parabolic mirror was simulated with Zemax OpticStudio [16], verify the correct optics and to have possible aberrations under control. The influence of the hole in the parabolic mirror on the laser beam was tested. As a first version, a Galileo telescope (no intermediate focus) was used before the beam transport in order to increase the beam diameter from the laser and to decrease the divergence and thus the expansion of the beam width over the long distance. Downstream of the beam transport (40 m), in the accelerator

hall, another telescope is used to get the desired beam width for the parabolic mirror to achieve the correct focal spot size at the IP.

### Background Measurement

To verify that the scattered photons can later be measured by the LEPS, a background measurement was made during the operation. The S-DALINAC was operated at 85 MeV electron energy, i.e., the energy amounted to 65 MeV in the third recirculation. In Fig. 3 the measured energy spectrum is shown in orange. The different peaks can be assigned to the calibration sources on the one hand and to radioactive background. In future experiments, the identified elements can be used for energy calibration. The blue line shows the Compton edge of the simulated LCB photons for the design source parameters. It is shown that the count rate of the scattered photons is three times higher than the background at this energy.

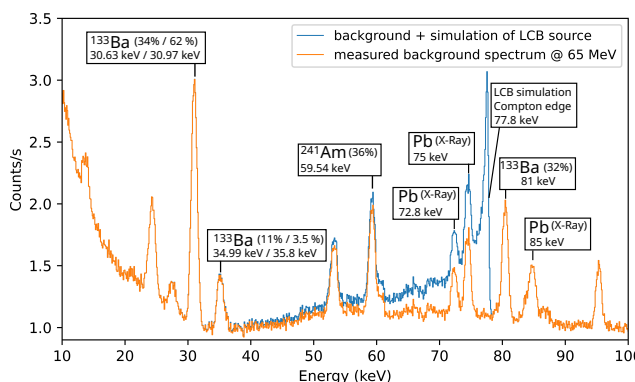


Figure 3: Energy spectrum, with measured background radiation during operation of S-DALINAC captured by LEPS (orange) and the same spectrum with simulated LCB beam hitting the detector at the same position (blue). As calibration sources  $^{133}\text{Ba}$  and  $^{241}\text{Am}$  were used.

## CONCLUSION

For this proposal all necessary analytical calculations were made and also a small simulation program was achieved. The design of the LCB Source is finalized and a selection of laser systems was made. The purchase of the laser system is currently in a tender process. A background radiation measurement in the accelerator hall was performed. It was successfully demonstrated by comparison with simulations of the LCB source, that the detection of the scattered photons will be possible. With this final design it will be possible to generate photons with energies up to about 180 keV at a bandwidth of  $\geq 0.6\%$  with a photon flux ranging from 10 Ph/s at collimation angle of 100  $\mu\text{rad}$  for the lowest bandwidth with up to  $2.4 \times 10^3$  Ph/s in an collimation angle of 1 mrad at a bandwidth of 2.9%. Based on these results, the individual components are now purchased and installed. A first test run is planned for next year.

## REFERENCES

- [1] K. Achterhold *et al.*, “Monochromatic computed tomography with a compact laser-driven X-ray source”, *Scientific Reports*, vol. 3, p. 1313, 2013. doi:10.1038/srep01313
- [2] E. Eggl *et al.*, “X-ray phase-contrast tomosynthesis of a human ex vivo breast slice with an inverse Compton x-ray source”, *Europhysics Letter*, vol. 116, p. 68003, 2016. doi:10.1209/0295-5075/116/68003
- [3] A. Zilges *et al.*, “Photonuclear reactions-From basic research to applications”, *Prog. Part. Nucl. Phys.*, vol. 122, p. 103903, 2022. doi:10.1016/j.ppnp.2021.103903
- [4] M. Peck *et al.*, “Performance of a twin position-sensitive Frisch-grid ionization chamber for photofission experiments”, *EPJ Web Conf.*, vol. 239, p. 05011, 2020. doi:10.1051/epjconf/202023905011
- [5] G. A. Krafft and G. Priebe, “Compton sources of electromagnetic radiation”, *Rev. Accel. Sci. Technol.*, vol. 03, p. 147, 2010. doi:10.1142/9789814340397\_0008
- [6] B. Günther *et al.*, “The versatile X-ray beamline of the Munich Compact Light Source: design, instrumentation and applications”, *J. Synchrotron Rad.*, vol. 27, pp. 1395-1414, 2020. doi:10.1107/S1600577520008309
- [7] T. Akagi *et al.*, “Narrow-band photon beam via laser Compton scattering in an energy recovery linac”, *Phys. Rev. Accel. Beams*, vol. 19, p. 114701, 2016. doi:10.1103/PhysRevAccelBeams.19.114701
- [8] R. Klein *et al.*, “Beam diagnostics at the BESSY I electron storage ring with Compton backscattered laser photons: measurement of the electron energy and related quantities”, *Nucl. Instr. And Meth. in Phys. Res. A*, vol. 384, p. 293, 1997. doi:10.1016/S0168-9002(96)00899-6
- [9] C. Sun *et al.*, “Energy and energy spread measurements of an electron beam by Compton scattering method”, *Phys. Rev. ST Accel. Beams*, vol. 12, p. 062801, 2009. doi:10.1103/PhysRevSTAB.12.062801
- [10] C. Chang *et al.*, “First Results of Energy Measurements with a Compact Compton Backscattering Setup at ANKA”, in *Proc. IPAC'15*, Richmond, VA, USA, May 2015, pp. 876-878. doi:10.18429/JACoW-IPAC2015-MOPHA040
- [11] M. Arnold *et al.*, “First operation of the superconducting Darmstadt linear electron accelerator as an energy recovery linac”, *Phys. Rev. Accel. Beams*, vol. 23, p. 020101, 2020. doi:10.1103/PhysRevAccelBeams.23.020101
- [12] C. Curatolo *et al.*, “Analytical description of photon beam phase spaces in inverse Compton scattering sources”, *Phys. Rev. Accel. Beams*, vol. 20, p. 080701, 2017. doi:10.1103/PhysRevAccelBeams.20.080701
- [13] R. Hajima and M. Fujiwara, “Narrow-band GeV photons generated from an x-ray free-electron laser oscillator”, *Phys. Rev. Accel. Beams*, vol. 19, p. 020702, 2016. doi:10.1103/PhysRevAccelBeams.19.020702
- [14] F. Schließmann *et al.*, “Realization of a multi-turn energy recovery accelerator”, submitted for publication
- [15] Pressemitteilung des Informationsdienst Wissenschaft (idw.), “Technologischer Durchbruch bei Energieeffizienten Teilchenbeschleunigern”, MI-NR. 63/2021, acc/feu. <https://idw-online.de/de/news776443/>.
- [16] Zemax, LLC, a Delaware limited liability company (ZEMAX): OpticStudio (Version 22.1.2) [Software] Available from <https://www.zemax.com/pages/opticstudio>, (01.06.2022).